Contribution from the Department of Chemistry,
Purdue University, West Lafayette, Indiana 47907

Intramolecular Electron Transfer at Metal Surfaces. 2. Comparisons of Ligand-Bridged Chromium(III) Reduction Kinetics at Silver vs. Mercury Electrodes

KENDALL L. GUYER[1] and MICHAEL J. WEAVER*

Received October 25, 1983

Rate parameters have been gathered for the electroreduction of a number of Cr(III) complexes attached to silver electrodes via one or more thiocyanate, azide, chloride, or bromide bridging ligands. Unimolecular rate constants k_{et} (s^{-1}) for electron transfer within the adsorbed state, as well as the surface concentration of the adsorbates, were obtained directly by using rapid linear sweep voltammetry. These data are also compared with corresponding kinetics and adsorption measurements at mercury electrodes in order to deduce the structural factors responsible for the substantially greater overall reactivities (i.e., larger apparent rate contents k_{app}) seen at silver. Marked differences in k_{et}, as well as k_{app}, were found between silver and mercury surfaces, these differences being sensitive to the nature of the nonbridging as well as the bridging ligands. This indicates that the metal surface exerts a significant influence upon the energetics of the elementary electron-transfer step as well as upon the stability of the precursor intermediate. Explanations for the observed structural influences upon k_{et} are sought in terms of "electronic communication" effects between the redox center and the metal surface.

Introduction

As noted in part 1 of this series,[2] we have undertaken a systematic study of measurements of the electrochemical reactivities of surface-attached reactants in order to explore in detail the nature and extent to which specific reactant–surface interactions can influence the kinetics of simple electron-transfer reactions at metal surfaces. The overall rationale behind the experimental strategies and choice of systems was summarized in part 1. In that article,[2] we examined the consequences of attaching various Co(III) ammine and ethylenediamine complexes to platinum and gold surfaces via halide and thiocyanate ligands on the kinetics of their one-electron reduction. A novel strategy was employed that entailed comparing unimolecular rate constants k_{et} (s^{-1}) for surface-attached (inner-sphere, k_{et}^{is}) and unattached (outer-sphere, k_{et}^{os}) reaction pathways, the latter being estimated from the conventional apparent rate constants k_{app} (cm s^{-1}) and from homogeneous outer-sphere rate data by using an "encounter preequilibrium" treatment.[3] The noticeable differences seen between corresponding values of k_{et}^{is} and k_{et}^{os} were rationalized in terms of the effects of reactant–surface interactions on the electron-transfer barrier.

Since such interactions should depend on the chemical nature of the electrode surface, the magnitude of k_{et}^{is} as well as k_{app} might be expected to be sensitive to the electrode material as well as the reactant structure. In order to explore this possibility further, we report here unimolecular rate constants for the one-electron reduction of various Cr(III) complexes bound to silver electrodes via isothiocyanate, azide, chloride, or bromide ligands. These data are compared with corresponding data for the same reactions occurring via both inner- and outer-sphere pathways at mercury in order to explore the factors responsible for the markedly greater overall reactivities (i.e., larger values of k_{app}) seen at the silver surface. This provides an illustrative comparison of reaction energetics at relatively electrocatalytic and noncatalytic surfaces.

Silver provides an especially interesting and tractable electrode material for such studies. By suitable pretreatment one may obtain a smooth and relatively clean surface that is ideally polarizable between ca. +150 and −700 mV vs. SCE at pH 3, at which unusually reproducible kinetic data can be obtained.[4-6] Since the effective potential of zero charge (pzc) for polycrystalline silver is extremely negative (−950 mV vs. SCE),[7] the surface promotes very strong specific adsorption of anions, metal complexes, and dipolar ligands.[5-8] This enables measurements of k_{et} to be obtained for a large variety of transition-metal reactants. In addition, for several of the present Cr(III) reactants, it proved possible to obtain values for the stability constants, K_p, for forming the adsorbed "precursor" state from the bulk reactant over a range of adsorbate coverages, enabling further insight to be obtained into the influence of reactant–electrode binding on k_{et}.

Electrochemical adsorbates at the silver surface are also of considerable current interest as prototype systems for the study of surface-enhanced Raman spectroscopy (SERS). A related study of the vibrational properties of several adsorbed Cr(III) reactants obtained by using SERS is presented elsewhere.[9]

Experimental Section

The various Cr(III) and Co(III) complexes used here were synthesized as outlined in ref 10–12. The electrolytes employed for the electrochemical measurements at silver were 0.1 M $NaClO_4$ + 2–10 mM $HClO_4$. (The acid was added to suppress formation of hydroxo complexes and to prevent the precipitation of $Cr(OH)_2$ on the electrode surface.) The sodium perchlorate was recrystallized twice from material that had been prepared from solid Na_2CO_3 and 60% $HClO_4$. Water was purified by an initial distillation of tap water from alkaline permanganate solution, followed by passage through an all-quartz "nonboiling" still (Dida-Sciences, Montreal).

Most of the procedures and apparatus employed have been detailed in earlier papers from this laboratory.[4,5] The silver electrodes were fabricated as rotating disks and were pretreated by electropolishing in a cyanide medium as outlined in ref 4 and 7a.

Measurements of apparent rate constants, k_{app}, for diffusing reactants at silver were obtained mostly by using rotating disk vol-

---

(1) Graduate Research Assistant, Michigan State University, 1977–1981.

(2) Barr, S. W.; Weaver, M. J. *Inorg. Chem.*, preceding paper in this issue.

(3) Hupp, J. T.; Weaver, M. J. *J. Electroanal. Chem. Interfacial Electrochem.* **1983**, *152*, 1.

(4) Barr, S. W.; Guyer, K. L.; Weaver, M. J. *J. Electroanal. Chem. Interfacial Electrochem.* **1980**, *111*, 41.

(5) Guyer, K. L.; Barr, W. W.; Cave, R. J.; Weaver, M. J. "Proceedings of the 3rd Symposium on Electrode Processes"; Bruckenstein, S., McIntyre, J. D. E., Miller, B., Yeager, E., Eds.; Electrochemical Society: Pennington, NJ, 1980; p 390.

(6) Guyer, K. L. Ph.D. Thesis, Michigan State University, 1981.

(7) (a) Larkin, D.; Guyer, K. L.; Hupp, J. T.; Weaver, M. J. *J. Electroanal. Chem. Interfacial Electrochem.* **1982**, *138*, 401. (b) Hupp, J. T.; Larkin, D.; Weaver, M. J. *Surf. Sci.* **1983**, *125*, 429.

(8) Guyer, K. L.; Barr, S. W.; Weaver, M. J. "Proceedings of the Symposium on Electrocatalysis"; O'Grady, W. E., Ross, P. N. Jr., Will, F. G., Eds.; Electrochemical Society: Pennington, NJ, 1982; p 377.

(9) Tadayyoni, M. A.; Farquharson, S.; Li, T. T-T.; Weaver, M. J. *J. Phys. Chem.*, in press. The utilization of SERS to monitor electrochemical kinetics involving such adsorbed species is described in: Farquharson, S.; Milner, D.; Tadayyoni, M. A.; Weaver, M. J. *J. Electroanal. Chem. Interfacial Electrochem.*, in press.

(10) Weaver, M. J.; Anson, F. C. *J. Electroanal. Chem. Interfacial Electrochem.* **1975**, *58*, 95.

(11) Weaver, M. J.; Satterberg, T. L. *J. Phys. Chem.* **1977**, *81*, 1772.

(12) Satterberg, T. L.; Weaver, M. J. *J. Phys. Chem.* **1978**, *82*, 1784.

0020-1669/84/1323-1664$01.50/0

Table I. Representative Rate Parameters for the Monobridged Inner-Sphere Reduction of Various Cr(III) Complexes at Silver and Mercury Electrodes at −600 mV vs. SCE at 24 °C

complex	surface	C_r,[a] mM	$10^{11}\Gamma_p$,[b] mol cm^{-2}	k_{app},[c] cm s^{-1}	α_{app}[d]	k_{et},[e] s^{-1}	α_{et}[f]
$Cr(NH_3)_5NCS^{2+}$	Ag		15^{g}			10.5^{m}	0.4
	Ag	0.9	$\sim25^{g,h}$	6×10^{-4} ^{m}	0.45^{m}	(2)	
	Hg	1.0	$2^{h,i}$	1.0×10^{-5} ^{l}	0.45^{l}	(0.5)	
$Cr(OH_2)_5NCS^{2+}$	Ag		20^{g}			20^{m}	0.35
	Ag	0.85	$\sim25^{g,h}$	1.2×10^{-3}	0.4^{m}	(4)	
	Hg	1.0	$0.5^{h,j}$	7.5×10^{-4}	0.4^{k}	(150)	
$Cr(NH_3)_5N_3{}^{2+}$	Ag	1.0	$\lesssim10^{g}$	$\lesssim10^{-5}$ ^{m}			
	Hg	1.0	$0.05^{h,j}$	5×10^{-7} ^{k}		(1.0)	
$Cr(OH_2)_5N_3{}^{2+}$	Ag		10^{g}			10^{m}	0.5
	Ag	0.95	$\sim20^{g,h}$	3×10^{-3} ^{m}	0.7^{m}	(~10)	
	Hg	1.0	$0.02^{h,j}$	2.0×10^{-5} ^{k}	0.55	(100)	
$Cr(NH_3)_5Cl^{2+}$	Ag	0.25	$\sim1\text{–}5^{h,j}$	1.3×10^{-2} ^{m}	0.7^{m}	(~100)	
	Hg	1.0	$\sim0.1^{h,j}$	1.0×10^{-5} ^{k}	0.5^{k}	(~10)	
$Cr(OH_2)_5Cl^{2+}$	Ag	0.25		$\sim0.3^{m}$			
	Hg	0.1	$\sim0.1^{h,j}$	1.5×10^{-3} ^{k}	0.35	($\sim1.5 \times 10^{3}$)	
$Cr(NH_3)_5Br^{2+}$	Ag	1.0		$\sim0.1^{m}$			
	Hg	1.0	$\sim0.3^{h,j}$	6×10^{-3} ^{k}	0.4	($\sim2 \times 10^{3}$)	
$Cr(OH_2)_5Br^{2+}$	Ag	0.25		$>0.5^{m}$			
	Hg	1.0		$\sim2.5^{k}$			

[a] Reactant concentration, corrected for diffusion polarization (i.e., just outside the diffuse layer) at −600 mV vs. SCE. [b] Surface reactant concentration at −600 mV, determined or estimated as noted. [c] Apparent rate constant at −600 mV, determined by using normal-pulse polarography and/or rotating disk voltammetry from $k_{app} = i_c/FC_r$, where i_c is the cathodic faradaic current density at −600 mV corresponding to the value of C_r listed. [d] Apparent transfer coefficient in the vicinity of −600 mV, determined from $\alpha_{app} = -(RT/F)(\mathrm{d}\ln k_{app}/\mathrm{d}E)$. [e] Rate constant for elementary electron-transfer step at −600 mV, from $k_{et} = i_c/F\Gamma_r$. Values without parentheses determined directly by using rapid linear sweep voltammetry (see text). Values inside parentheses (k_{et}^{est}) obtained from corresponding listed values of k_{app} and K_p ($=\Gamma_p/C_r$) by using $k_{et}^{est} = k_{app}/K_p$. [f] Transfer coefficient for elementary electron-transfer step in vicinity of −600 mV, determined from $\alpha_{et} = -(RT/F)(\mathrm{d}\ln k_{et}/\mathrm{d}E)$. [g] Determined from rapid linear sweep voltammetry. [h] Extrapolated from adsorption data at less negative potentials and/or from smaller values of C_r (see Table III and ref 18). [i] Determined from single-step chronocoulometry (ref 18 and 19). [j] Estimated by using a "kinetic probe" technique (see text and ref 6 and 18). [k] Determined in 1 M $NaClO_4$ (pH 2-3). [l] Determined in 40 mM $La(ClO_4)_3$ (pH 2-3). [m] Determined in 0.1 M $NaClO_4$ (pH 2.5).

tammetry[4] and/or normal-pulse polarography with a rotated electrode, using a PAR 174 polarographic analyzer (EG & G Instruments, Inc.). The bulk reactant concentrations were normally 0.5–2 mM. With the latter technique, it was found to be necessary to spin the electrode in order to completely replenish the diffusion layer between consecutive potential pulses. With a pulse time of 50 ms, delay periods of 2–5 s between pulses, and rotation speeds in the range 250–1000 rpm, this reactant-depletion effect was found to be entirely eliminated without significantly influencing the propagation of the diffusion layer during each potential pulse. Measurements of k_{app} at mercury surfaces were made by using normal-pulse polarography with a dropping-mercury electrode having a mechanically controlled drop time of 2 s. The kinetic analysis of the resulting current–potential data utilized the procedure of Oldham and Parry.[13] The kinetic data analysis for rotating disk voltammograms of irreversible electrode reactions have been described previously.[4,5] The majority of the reactions were found to be totally irreversible under the conditions of rotating disk voltammetry and normal-pulse polarography in that cathodic–anodic cyclic voltammograms yielded anodic [Cr(II) reoxidation] peaks only at potentials well positive of the range where the cathodic rate parameters were measured. However, the reductions of $Cr(OH_2)_5Cl^{2+}$ and $Cr(OH_2)_5Br^{2+}$ are sufficiently rapid to require substantial corrections for anodic back-reactions. This can create a difficulty since the predominant anodic reaction is $Cr^{2+} + X^- (Cl^-, Br^-) - e^- \rightarrow CrX^{2+}$, i.e., is first order in *both* Cr^{2+} and X^-, which severely complicates the application of the usual back-reaction corrections.[14,15] This difficulty was circumvented by adding a small excess (2–5 mM) of chloride or bromide ions, as appropriate, so that the anodic reaction became pseudo-first-order overall. Rate constants at the effective "formal potential" of the Cr(III)/Cr(II) redox couple were determined from the cathodic–anodic peak separation for the resulting quasi-reversible cyclic voltammograms.[16]

The procedure for determining k_{et} for adsorbed reactants using fast linear sweep voltammetry is described in the Results. Equipment utilized included a programmable voltage ramp generator of in-house design, a PAR Model 173 potentiostat with Model 179 plug-in module, and a Tektronix 7623A storage oscilloscope with a Polaroid camera. The chronocoulometric measurements utilized an on-line data acquisition and analysis system based on a LSI-11 microcomputer, along with a fast potentiostat of in-house design. Data acquisition was typically 200 points at a rate of 20 kHz.

All electrode potentials were measured with respect to the saturated calomel electrode (SCE), and all electrochemical measurements were performed at 24 ± 0.5 °C.

Results

Apparent Inner-Sphere Reactivities. Table I contains a summary of electrochemical rate parameters for the reduction of various pentaaquo- and pentaamminechromium(III) complexes, each containing a single potential bridging anion, at the polycrystalline silver–aqueous 0.1 M $NaClO_4$ interface. The overall rate data are summarized as values of the apparent rate constant k_{app} measured at −600 mV vs. SCE along with the corresponding apparent transfer coefficients α_{app} [$=-(RT/F)(\mathrm{d}\ln k_{app}/\mathrm{d}E)$] at the same potential. Since the Tafel ($\ln k_{app}$ vs. E) plots are roughly linear over the ca. 200–300 mV range of overpotentials that are normally accessible, these two parameters suffice to describe the overall kinetic behavior for each reaction. Also listed for each reactant are the corresponding rate parameters determined previously at the mercury–aqueous interface,[11,14,17] also measured at −600 mV. (This electrode potential was chosen for comparison so

---

(13) Oldham, K. B.; Parry, E. P. *Anal. Chem.* **1968**, *40*, 65.

(14) (a) Weaver, M. J.; Anson, F. C. *Inorg. Chem.* **1976**, *15*, 1871. (b) Weaver, M. J.; Anson, F. C. *J. Am. Chem. Soc.* **1975**, *97*, 4403.

(15) Weaver, M. J.; Anson, F. C. *J. Electroanal. Chem. Interfacial Electrochem.* **1975**, *65*, 711.

(16) Nicholson, R. S. *Anal. Chem.* **1965**, *37*, 1351.

(17) A smaller ionic strength of supporting electrolyte was utilized for the kinetics measurements at silver (0.1 M) than at mercury (1 M) in order to diminish the concentration of the ionic and other contaminants at the strongly adsorbing silver surface. Nevertheless, the alteration of the supporting electrolyte from 1 to 0.1 M $NaClO_4$ yielded only small (ca. 50%) increases in k_{app} for the reduction of the Cr(III) complexes at mercury at −600 mV, in accordance with the anticipated double-layer effects.[14]

(18) Weaver, M. J. *Inorg. Chem.* **1979**, *18*, 402.

(19) Frank, S. N.; Anson, F. C. *J. Electroanal. Chem. Interfacial Electrochem.* **1974**, *54*, 55.

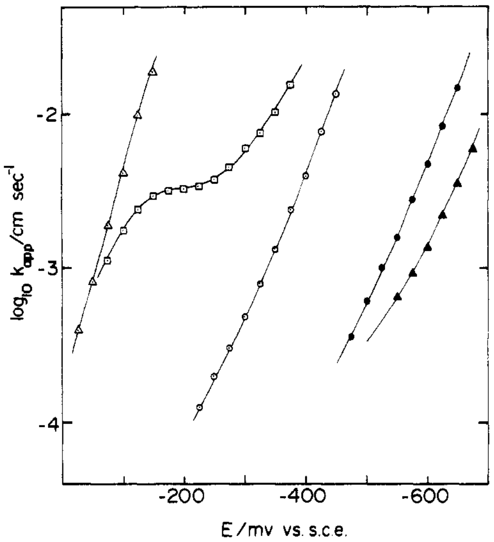

Figure 1. Logarithm of the apparent rate constant for the electroreduction of $Co(NH_3)_5F^{2+}$ (open symbols) and $Cr(NH_3)_5Cl^{2+}$ (closed symbols) at silver plotted against the electrode potential: circles, obtained in 0.1 M $NaClO_4$ + 2 mM $HClO_4$; squares and triangles, obtained after the addition of 0.02 and 1 mM NaCl, respectively.

to minimize the extent of ln k_{app}–E data extrapolation that was required.)

These rate data at mercury surfaces have been shown to refer uniformly to anion-bridged reduction pathways.[11,14] Each of the eight reactions at silver given in Table I is also believed to follow an inner-sphere pathway. This mechanistic assignment is based on several lines of evidence. First, several complexes [$Cr(NH_3)_5NCS^{2+}$, $Cr(OH_2)_5NCS^{2+}$, $Cr(OH_2)_5N_3^{2+}$] were found to specifically adsorb to a detectable amount at silver by using rapid linear sweep voltammetry (vide infra) even at very small bulk concentrations ($\lesssim 10$ μM). This direct detection of the precursor intermediate certifies an inner-sphere mechanism in that rates for reaction within the adsorbed state can be obtained directly.[10] The chloride and bromide ligands do not induce sufficient reactant adsorption to allow mechanism diagnoses in this manner. However, strong evidence in favor of inner-sphere reduction mechanisms for the halide-, as well as the isothiocyanate- and azide-containing complexes, is deduced from the observation that the values of k_{app} at a given electrode potential generally decreased upon addition of adsorbing nonreacting anions. This contrasts with the rate increases expected on electrostatic grounds for such cationic complexes reacting via outer-sphere mechanisms.[11,12,14] This method has been utilized previously to distinguish between inner- and outer-sphere mechanisms for the electroreduction of cationic Cr(III) and Co(III) complexes at mercury[11,12,14] and of Co(III) ammines at platinum and gold surfaces.[2,5] The observed rate decreases appear to arise from destabilization of the inner-sphere transition state caused by repulsive interactions with the nonreacting adsorbed anions[11,12,14]or, in the case of the solid metals, from elimination of surface coordination sites.[2,5]

Some typical results of this type obtained at silver electrodes are illustrated in Figure 1. The open symbols are log k_{app}–E (Tafel) plots obtained for $Co(NH_3)F^{2+}$ reduction, and the closed symbols are those for $Cr(NH_3)_5Cl^{2+}$ reduction. The circles represent the Tafel plots obtained in 0.1 M $NaClO_4$ + 2 mM $HClO_4$. It is seen that the addition of 1 mM chloride (triangles) yields a striking increase (ca. 10^3-fold) in the values of k_{app} for $Co(NH_3)_5F^{2+}$ reduction. This is expected since the reaction probably occurs via an outer-sphere pathway;[4,5] chloride is strongly adsorbed under these conditions and yet is incapable of acting as a ligand bridge on account of the substitution inertness of Co(III) or Cr(III).[11,12] In contrast, the addition of 1 mM chloride under the same conditions yields marked rate decreases for the reduction of $Cr(NH_3)_5Cl^{2+}$ (Figure 1), suggesting an inner-sphere mechanism. Comparable rate decreases were observed for the other Cr(III) reduction reactions in Table I upon addition of chloride or other adsorbing nonreacting anions, indicating that these reactions also proceed via ligand-bridged pathways. Other evidence supporting these mechanistic assignments is provided by the observation that the values of k_{app} at −600 mV for each reactant are uniformly larger than the corresponding values obtained at mercury electrodes (Table I), even though the latter values have been shown to correspond to ligand-bridged pathways,[11,14] and the outer-sphere reduction of $Co(NH_3)_5F^{2+}$ and $Co(NH_3)_6^{3+}$ proceeds at similar rates on the two surfaces in perchlorate media.[4,5]

Attempts to measure the electroreduction kinetics of a number of Cr(III) complexes that are reduced more slowly than those in Table I, including $Cr(NH_3)_6^{3+}$, $Cr(NH_3)_5OH_2^{3+}$, $Cr(OH_2)_6^{3+}$, and $Cr(OH_2)_5NO_3^{2+}$ were thwarted by the onset of current due to proton reduction, which occurs at potentials more negative of ca. −750 mV in the weakly acidic media (pH 2.5–3) employed here.

Determination of Reactant Specific Adsorption. Provided that electron transfer is rate controlling, we can relate the apparent rate constant for the overall reaction k_{app} to the unimolecular rate constant for the elementary electron-transfer step k_{et} by[3]

$$k_{et} = k_{app}/K_p \qquad (1)$$

The precursor stability constant K_p equals Γ_p/C_r, where Γ_p (mol cm^{-2}) is the surface concentration of the adsorbed reactant (precursor state) corresponding to a given reactant concentration C_r (mol cm^{-3}).

An indication that the adsorbed reactant concentration commonly approaches saturation at silver is provided by the observation that the apparent electrochemical reaction orders at a given electrode potential, $R_e = (\partial \ln i_c/\partial \ln C_r)_E$, are noticeably below unity.[2,6] For the thiocyanate-bridged processes, $R_e \lesssim 0.3$–0.5. Strong reactant adsorption is also implicated from the observation that the outer-sphere electroreduction rates of $Co(NH_3)_5F^{2+}$ and $Co(NH_3)_6^{3+}$ were significantly decreased (by 2- to 5-fold) upon addition of even small concentrations (0.01–1 mM) of these Cr(III) complexes within potential ranges that are positive (ca. −200 to −450 mV vs. SCE) of where the latter are reduced.[6] Such rate decreases presemably arise from repulsion between the cationic probe reactants and the cationic Cr(III) adsorbates.[6]

The conventional method for evaluating specific adsorption of electroactive species is potential-step chronocoulometry. Our initial attempts to determine the extent of adsorption for Cr(III) complexes at silver utilized single-step chronocoulometry. (The double-step variant is inapplicable for most of these systems on account of their chemical irreversibility.) However, the apparent adsorption Γ_{app} determined, as usual,[20] from the difference in the intercepts of the charge vs. square root of time (q–$t^{1/2}$) plots for a given potential step in the presence and absence of the adsorbate often yielded values of Γ_{app} that were unreasonably small or even negative.[6]

These difficulties led us to search for alternative Faradaic methods for determining the extent of reactant adsorption. One advantage of the present systems is that the majority of the reactants are sufficiently strongly adsorbed so that only small bulk concentrations (<10^{-4} M) are necessary in order to induce substantial amounts of reactant adsorption. This fact considerably eases the task of determining the adsorption using Faradaic means inasmuch as the Faradaic charge arising

---

(20) Anson, F. C. *Anal. Chem.* **1965**, *36*, 932.

Table II. Representative Adsorption Data for Various Cr(III) Complexes and Corresponding Free Anions at Silver and Mercury Electrodes at 24 °C

adsorbate	surface	electrolyte	potential, mV vs. SCE	C_r,[a] mM	$10^{11}\Gamma_p$,[b] mol cm^{-2}	K_p,[c] cm
$Cr(NH_3)_5NCS^{2+}$	Ag	0.1 M $NaClO_4$	−200	0.05	9.5^d	2×10^{-3}
		0.1 M $NaClO_4$	−200	0.10	16^d	1.5×10^{-3}
	Hg	0.32 M Na_2SO_4	−200	0.8	3.3^e	4×10^{-5}
$Cr(OH_2)_5NCS^{2+}$	Ag	0.1 M $NaClO_4$	−300	0.02	18^d	9×10^{-3}
			−150	0.02	13^d	6.5×10^{-3}
	Hg	0.5 M $NaClO_4$	−200	2	$\sim 3^f$	$\sim 1.5 \times 10^{-5}$
		0.5 M $NaClO_4$	−400	2	$\sim 2^f$	$\sim 1 \times 10^{-5}$
NCS^-	Ag	0.1 M $NaClO_4$	−200	0.001	$\sim 10^e$	~0.1
		0.1 M $NaClO_4$	−400	0.001	$\sim 10^e$	~0.1
	Hg	1 M KF	−200	0.1	$3^{g,h}$	3×10^{-4}
		1 M KF	−400	1.0	2.5^g	2.5×10^{-5}
$Cr(NH_3)_5N_3^{2+}$	Ag	0.1 M $NaClO_4$	−200	0.1	$<5^d$	$<5 \times 10^{-4}$
	Hg	1 M KF	−300	10	$\sim 2^f$	$\sim 2 \times 10^{-6}$
$Cr(OH_2)_5N_3^{2+}$	Ag	0.1 M $NaClO_4$	−300	0.04	4^d	1×10^{-3}
		0.1 M $NaClO_4$	−100	0.04	4^d	1×10^{-3}
	Hg	0.5 M $NaClO_4$	−300	10	<1	$<1 \times 10^{-6}$
N_3^-	Ag	0.5 M NaF	−200	0.1	$\sim 10^{g,h}$	$\sim 1 \times 10^{-3}$
		0.5 M NaF	−400	0.1	$\sim 5^g$	$\sim 5 \times 10^{-4}$
	Hg	0.95 M NaF	−400	25	5^g	2×10^{-6}
cis-$Cr(OH_2)_4(NCS)_2$	Ag	0.1 M $NaClO_4$	−200	0.4	11^d	3×10^{-3}
	Hg	1 M $NaClO_4$	−200	0.05	5^e	1×10^{-3}
		1 M $NaClO_4$	0	0.025	5^e	2×10^{-3}
fac-$Cr(OH_2)_3(NCS)_3$	Ag	0.1 M $NaClO_4$	−200	0.005	5^d	1×10^{-2}
		0.1 M $NaClO_4$	−200	0.075	14^d	2×10^{-3}
		0.1 M $NaClO_4$	−100	0.005	10^d	2×10^{-2}
	Hg	1 M $NaClO_4$	−200	0.03	5^e	1.5×10^{-3}
		1 M $NaClO_4$	0	0.0025	5^e	2×10^{-2}
$Cr(NCS)_6^{3-}$	Ag	0.1 M $NaClO_4$	−200	0.01	7^d	7×10^{-3}
		0.1 M $NaClO_4$	−200	0.08	15^d	2×10^{-3}
	Hg	1 M $NaClO_4$	−200	0.03	12^e	4.5×10^{-3}
		1 M $NaClO_4$	−400	0.15	10^e	6×10^{-4}
cis-$Cr(en)_2(NCS)_2^+$	Ag	0.1 M $NaClO_4$	−200	0.04	4.5^d	1×10^{-3}
		0.1 M $NaClO_4$	−500	0.04	3^d	7.5×10^{-4}
	Hg	0.32 M Na_2SO_4	−200	0.005	11^e	2.2×10^{-2}
		0.32 M Na_2SO_4	−500	0.005	9^e	1.8×10^{-2}

[a] Bulk reactant concentration. [b] Surface reactant concentration at stated electrode potential, determined by using method indicated. [c] Adsorption coefficient, equal to Γ_p/C_r. [d] Determined by using rapid linear sweep voltammetry (see text for details). [e] Determined by using single-step chronocoulometry (see ref 10 and 19). [f] Determined by using kinetic probe technique (see text and ref 6). [g] Determined by using capacitance measurements, from ref 7 (NCS^-), 23, and 24 (N_3^-). [h] Extrapolated value.

from the diffusing reactant can often be arranged to be negligibly small compared to that from the initially adsorbed species. This suggested that linear sweep voltammetry (LSV) could provide a means of determining the extent of reactant adsorption from the area underneath that cathodic current–time peak, provided that the sweep rate is suitably large so that the adsorbate reduction provides the predominant contribution to the overall Faradaic charge. Trial calculations indicate that this situation holds when $C_r < 10^{-4}$ M for sweep rates $v > 10$ V s^{-1}.[21] For example, where $v = 20$ V s^{-1}, $\Gamma_p = 2.5 \times 10^{-10}$ mol cm^{-2}, and $C_r = 10^{-4}$ M, more than 90% of the measured Faradaic charge is estimated to arise from the adsorbed reactant. This expectation was confirmed experimentally by obtaining cathodic voltammograms over a range of reactant concentrations for the reductions of $Cr(OH_2)_5NCS^{2+}$ and $Cr(NH_3)_5NCS^{2+}$, which are adsorbed at silver to extents approaching a monolayer even at very low bulk concentrations ($C_r \sim 10$ μM).

Some typical results for the reduction of *cis*-$Cr(OH_2)_4(NCS)_2^+$ adsorbed at silver and mercury electrodes are shown in Figure 2a,b. The voltammograms generally have an asymmetrical peak shape in accordance with theoretical expectations,[22] although those obtained at silver (and at other polycrystalline solid electrodes) were usually somewhat broader than expected.[6,22] Sweep rates in the range 10–50 V s^{-1} proved to be the most useful; distortions due to solution resistance became significant above ca. 50 V s^{-1}. The extent of adsorption was estimated from such voltammograms by integrating the area (charge) under the current–time peak, the base line being formed by a straight line drawn between the level current–potential segments on either side of the peak. (For some reactions, as in Figure 2a, the voltammetric peak was sufficiently close to the onset of hydrogen evolution that the shape of the current base line on the cathodic side of the peak had to be estimated). This procedure yields an "internal" correction for the influence of the adsorbate upon the double-layer capacitance in the region where the adsorbate is reduced. The values of Γ_p so derived were found to be essentially independent of the sweep rate in the range 10–50 V s^{-1}.

An alternative method, akin to that employed in single-step chronocoulometry, is to integrate the current–time curve between a suitable pair of potentials on either side of the peak and subtract the corresponding charge obtained between these potentials by using the same sweep rate in the absence of the adsorbate (i.e., from the dashed curve in Figure 2a). Interestingly, this latter method tended to yield unreasonably small estimates of Γ_p that approached the chronocoulometric values.[8] A key assumption contained in this type of analysis is that the average double-layer capacitance between the initial and final potentials is unaltered by the presence of the adsorbate.[20] This is likely to be invalid for the present systems since the free anions released upon reduction are strongly adsorbed even at the most negative potentials (ca. −750 mV) that can be em-

---

(21) Barr, S. W. Ph.D. Thesis, Michigan State University, 1981.

(22) Laviron, E. *J. Electroanal. Chem. Interfacial Electrochem.* **1974**, *52*, 355. Kozlowska, H. A.; Klinger, J.; Conway, B. E. *Ibid.* **1977**, *75*, 45.

(23) Weaver, M. J.; Anson, F. C. *J. Electroanal. Chem. Interfacial Electrochem.* **1975**, *65*, 737.

(24) Gonzalez, E. R. *J. Electroanal. Chem. Interfacial Electrochem.* **1978**, *90*, 431.

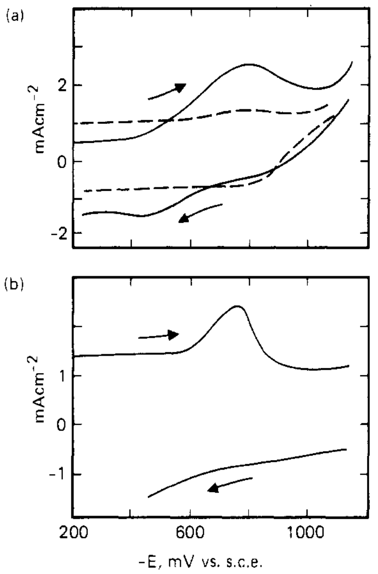

Figure 2. Cathodic–anodic cyclic voltammograms for the reduction of *cis*-$Cr(OH_2)_4(NCS)_2^+$ at (a) silver and (b) mercury electrodes. The sweep rate was 50 V s^{-1} in both cases. Other conditions: (a) 40 μM reactant in 0.1 M $NaClO_4$ + 2 mM $HClO_4$, initial potential −100 mV (dashed curve obtained in the absence of the reactant); (b) 80 μM reactant, otherwise the same as in (a).

ployed for the chronocoulometric steps.

The LSV method was used to obtain values of Γ_p corresponding to bulk concentrations C_r in the range 0.01–0.1 mM for each of the Cr(III) reactants listed in Table I as well as for *cis*-$Cr(OH_2)_4(NCS)_2^+$, *fac*-$Cr(OH_2)_3(NCS)_3$, $Cr(NCS)_6^{3-}$, and *cis*-$Cr(en)_2(NCS)_2^+$. Some representative results are summarized in Table II. The adsorption generally appeared to be reversible in that constant Γ values were obtained only a few seconds after addition of the adsorbate to a stirred solution and exhibited the same potential dependence irrespective of the direction in which the initial potential was altered. Also included for comparison are some pertinent adsorption data for the corresponding free anions at silver[7] and data for the same complexes and free anions obtained at mercury electrodes.[4] The entries in Table II were selected so that the adsorbate coverages are sufficiently below unity so that Henry's law is approximately obeyed; i.e., the values of K_p ($=\Gamma_p/C_r$) are roughly independent of Γ_p. Under these conditions K_p should reflect primarily adsorbate–electrode, rather than adsorbate–adsorbate interactions.

These adsorption data, obtained at potentials positive of the region where the complexes are reduced, were also utilized to obtain approximate estimates of Γ_p and hence K_p at −600 mV at the reactant concentrations for which the kinetic data in Table I were gathered. Extrapolations of the extent of adsorption to a more negative potential and larger values of C_r are necessarily required. However, this was facilitated by the observation (Table II) that the dependences of Γ_p on electrode potential at silver are relatively mild. Several complexes are reduced sufficiently rapidly at −600 mV so that the quoted value of k_{app} corresponds to a reactant concentration C_r well below the bulk value as a consequence of concentration polarization. Cognizance of this was taken in that the value of C_r and hence Γ_p corresponding to each value of k_{app} given in Tables I and II are those estimated to be present at the electrode surface from the magnitude of the measured current in relation to the diffusion-limited value.

The values of k_{app} given in Table I were then combined with the corresponding estimates of K_p ($=\Gamma_p/C_r$) at −600 mV (eq 1) to yield the values of k_{et} listed (in parentheses) in Table I and III.

Rate Constants for Adsorbed Reactants. LSV also provided a means of directly determining values of k_{et} for adsorbed reactants from the electrode potentials required for their reduction. Some direct determinations of k_{et} for thiocyanate-bridged Cr(III) reactants at mercury electrodes using chronocoulometry have been reported previously.[10] The approach used in this earlier study is similar to the present one in that sufficiently dilute reactant concentrations were used so that the observed Faradaic current arises overwhelmingly from reduction of the initially adsorbed reactant. This circumstance, necessary for the straightforward analysis of kinetic data for adsorbed reactants,[10] was facilitated by the tenacious adsorption found at silver surfaces even for monobridged complexes (Table II).

A series of cathodic–anodic cyclic voltammograms were recorded from a given initial potential by using sweep rates in the range 5–50 V s^{-1}. Plots of the surface rate constant k_{et} as a function of overpotential were obtained in two ways. The first method involved determining the adsorbate concentration Γ' remaining at a series of points within a given current–potential transient. The surface rate constant k_{et} at each potential was calculated from the instantaneous Faradaic current density i_c at this point from $k_{et} = i_c/F\Gamma'$. This analysis therefore assumes that the reaction is first order in the adsorbed reactant. An alternative method that avoided this assumption involved computing k_{et} for a fixed adsorbate concentration at different electrode potentials by utilizing linear sweep voltammograms at several sweep rates. The two methods generally yielded log k_{et}–E plots that were in reasonable agreement (values of k_{et} within ca. 50%). Representative values of k_{et}, along with the values of Γ_p to which they refer, are listed in Table I. Note that these directly measured values of k_{et} are listed without parentheses; this is to distinguish them from the estimates obtained indirectly from k_{app} and K_p that are given in parentheses. In the ensuing discussion, we shall refer to these two sets of surface rate constants as k_{et} and k_{et}^{est}, respectively. Estimates of the potential dependence of k_{et}, expressed as α_{et} [$=-(RT/F)(\mathrm{d}\ln k_{et}/\mathrm{d}E)$], are also given in Table I.

Values of k_{et} were also determined for the electroreduction of a number of adsorbed Cr(III) and Co(III) complexes containing two or more isothiocyanate ligands in the cis position. Such complexes are of particular interest since the exposed sulfur linkages provide sufficiently strong adsorption at mercury electrodes to allow values of k_{et} to be directly measured at this surface[10] as well as at silver electrodes. Representative values of k_{et} for the reduction of five such adsorbates at silver and mercury electrodes are given in Table III, again with the values of Γ_p to which they refer. The values of k_{et} at mercury electrodes were also determined by using LSV; these results were found to be closely similar to those obtained under comparable conditions by using chronocoulometry.[10]

Values of both k_{et} and k_{et}^{est} could be obtained at silver surfaces for four reactions in Tables I and III. It is seen that k_{et} is typically 2- to 5-fold larger than the corresponding indirect estimates k_{et}^{est}. Although these differences are not large, they are considered to beyond experimental error. This suggests that there are significant differences in the nature of the average adsorption sites involved in the overall steady-state reaction to which k_{app} and hence k_{et}^{est} refer, from the transient reduction of the previously equilibrated adsorbate to which k_{et} refers. The rate of precursor-state formation may be sufficiently slow, at least at certain sites on the polycrystalline surface, so that these sites are unable to contribute significantly to the rate of the overall reaction, thereby diminishing k_{et}^{est} relative to k_{et}.

Discussion

Comparison of Inner-Sphere Reactivities at Silver and Mercury Surfaces. The kinetics and adsorption data for the

Table III. Representative Intramolecular Rate Parameters for the Multibridged Inner-Sphere Reduction of Various Cr(III) and Co(III) Complexes at Silver and Mercury Electrodes in 0.1 M $NaClO_4$ at 24 °C[a]

complex	surface	electrode potential, mV vs. SCE	$10^{11} \times \Gamma_p$,[b] mol cm^{-2}	k_{et},[e] s^{-1}	α_{et}[f]
cis-$Cr(OH_2)_4(NCS)_2^+$	Ag	−600	11	50	0.35
	Hg	−600	4	70	0.45
fac-$Cr(OH_2)_3(NCS)_3$	Ag	−600	7	100	~0.4
	Hg	−600	10	70	0.35
$Cr(NCS)_6^{3-}$	Ag	−600	14	160	~0.3
	Hg	−600	11	15	~0.4
cis-$Cr(en)_2(NCS)_2^+$	Ag	−800	5	30	0.45
	Hg	−800	10	2	0.45
cis-$Co(en)_2(NCS)_2^+$	Ag	−100	10	40	~0.5
	Ag	−100	21	(22)	
	Hg	−100	6	0.15	~0.6

[a] For key, see footnotes to Table I.

monobridged Cr(III) reductions in Tables I and II clearly show that the markedly enhanced overall reactivity, i.e. the larger values of k_{app}, for most reactions at silver compared to the corresponding reactivities at mercury is due in part to larger values of K_p, i.e. to the uniformly greater concentrations of the adsorbed intermediates at the former surface. Thus, the ca. 2- to 10^3-fold larger values of k_{ap} at silver electrodes are mirrored by values of K_p that also are up to 10^3-fold larger (Table III).

Although the number of suitable reactant systems is not large, some interesting reactivity trends can nonetheless be discerned. The ratios $(k_{app}^{Ag}/k_{app}^{Hg})_E$ of apparent rate constants for a given reaction on silver compared to mercury are sensitive not only to the nature of the bridging ligand X but also to the nonbridging ligands L in that this ratio is uniformly smaller when L = OH_2 than when L = NH_3. Also, these bridging and nonbridging ligand effects are attributable only in part to differences in the extent of reactant adsorption since the corresponding ratios of surface rate constants $(k_{et}^{Ag}/k_{et}^{Hg})_E$ also generally differ from unity and depend upon both X or L.

In order to understand these reactivity differences, it is useful to express k_{et} in terms of the reorganization energy for the elementary electron-transfer step ΔG_{et}^*[2,3]

$$k_{et} = \kappa_{el}\nu_n \exp(-\Delta G_{et}^*/RT) \qquad (2)$$

where κ_{el} is the electronic transmission coefficient (i.e. the electron tunneling probability within the transition state) and ν_n is the nuclear frequency factor. The former should approach unity (i.e., adiabaticity is achieved) for inner-sphere reactions involving small inorganic bridges.[25] The latter is expected to be close to 1×10^{13} s^{-1} for the present reactions.[3,25] The reorganization energy can also be separated into an intrinsic barrier, ΔG_{int}^*, and a "thermodynamic" contribution, ΔG_{et}°, according to[2,18]

$$\begin{aligned}\Delta G_{et}^* &= \Delta G_{int}^* + \alpha_{et}[F(E - E^\circ) + RT(\ln K_p - \ln K_s)] \\ &= \Delta G_{int}^* + \alpha_{et}\Delta G_{et}^\circ\end{aligned} \qquad (3)$$

where α_{et} is the transfer coefficient for the electron-transfer step (≈0.5), E° is the standard (or formal) potential for the reacting redox couple and K_p and K_s are the equilibrium constants for forming the precursor and successor states from the bulk reactant and product, respectively. (See ref 2 and 18 for further comments on these relations.)

The closely related reactants $Cr(OH_2)_5NCS^{2+}$, $Cr(OH_2)_5N_3^{2+}$, and $Cr(NH_3)_5NCS^{2+}$ form an interesting comparison. The larger values of k_{app} for $Cr(OH_2)_5NCS^{2+}$ compared with those for $Cr(OH_2)_5N_3^{2+}$ reduction at a given electrode surface are largely accounted for by differences in K_p so that k_{et}^{est} is approximately the same for these two reactants (Table I). This finding is expected since $-N_3^-$ and $-NCS^-$ should present a similar coordination environment to the chromium redox center.[18] However, the values of k_{et}^{est} for both $Cr(OH_2)_5NCS^{2+}$ and $Cr(OH_2)_5N_3^{2+}$ reduction are smaller at silver compared with those at mercury by factors of ca. 40 and 10, respectively. In contrast, k_{et}^{est} for $Cr(NH_3)_5NCS^{2+}$ reduction at silver is slightly larger than that at mercury (Table I).

A clue to the origin of these behavioral differences is provided by the observation that the ratio of k_{et}^{est} values, $(k_{et}^{OH_2}/k_{et}^{NH_3})_E$, for $Cr(OH_2)_5NCS^{2+}$ and $Cr(NH_3)_5NCS^{2+}$ reduction at a given surface is much larger at mercury (300) than at silver (2). The latter rate ratio is unexpected on the basis of both overall thermodynamic and intrinsic factors.[27] Indeed reactivity ratios of ca. 50–500 have been found for the homogeneous inner-sphere reduction of several corresponding $Cr(OH_2)_5X^{2+}$ and $Cr(NH_3)_5X^{2+}$ complexes by Cr^{2+} [28] and Yb^{2+}.[29] It therefore appears that the pentaaquochromium(III) complexes experience reorganization barriers ΔG_{et}^* (eq 2) at the silver surface that are unexpectedly large.

Such nonbridging ligand effects on the relative reorganization barriers at silver and mercury surfaces are also present for the multibridged reductions in Table III. Thus, the reactivity ratio $(k_{et}^{Ag}/k_{et}^{Hg})_E$ increases from 0.7 to 15 when the four aquo ligands in *cis*-$Cr(OH_2)_4(NCS)_2^+$ are replaced by two ethylenediamines; this rate ratio is also large (250) for *cis*-$Co(en)_2(NCS)_2^+$ reduction (Table III). Stepwise replacements of the aquo ligands in $Cr(OH_2)_5NCS^{2+}$ by two, three, or six $-NCS^-$ anions lead to marked increases in $(k_{et}^{Ag}/k_{et}^{Hg})$, from ca. 0.03 (Table I) to 10 (Table III). Generally then, the silver surface induces noticeably larger values of k_{et} than at mercury for reactants containing ammine, ethylenediamine, and thiocyanate nonbridging groups, whereas the opposite is true for complexes containing aquo ligands.

These substrate effects upon k_{et} appear to arise in part from differences in the thermodynamic (ΔG_{et}°) as well as intrinsic (ΔG_{int}^*) components of ΔG_{et}^* for a given reaction at silver and mercury. This can be seen by expressing the unimolecular rate ratio $(k_{et}^{Ag}/k_{et}^{Hg})_E$ in the form

$$\begin{aligned}RT \ln (k_{et}^{Ag}/k_{et}^{Hg})_E = (\Delta G_{i,Hg}^* - \Delta G_{i,Ag}^*) - \\ \alpha_{et}RT[\ln (K_p^{Ag}/K_p^{Hg})_E - \ln (K_s^{Ag}/K_s^{Hg})_E]\end{aligned} \qquad (4)$$

where the subscripts and superscripts "Ag" and "Hg" again refer to parameters determined at silver and mercury surfaces. Values of K_s cannot be measured for the present systems on account of the substitution lability of Cr(II) and Co(II).

---

(25) Support for these assertions is provided by the observation that unimolecular frequency factors, $\kappa_{el}\nu_n$, close to 1×10^{13} s^{-1} are obtained for several thiocyanate-bridged reactions at mercury electrodes from the dependence of k_{et} on temperature.[26]

(26) Li, T. T-T.; Barr, S. W.; Guyer, K. L.; Weaver, M. J. *J. Electroanal. Chem. Interfacial Electrochem.* **1984**, *164*, 27.

(27) Although the standard potentials for $Cr(OH_2)_5NCS^{2+/+}$ and $Cr(NH_3)_5NCS^{2+/+}$ are unknown, since ammonia should form more stable complexes with Cr(III) than with Cr(II) it is likely that E° for the latter complex would be significantly more negative, yielding a less favorable thermodynamic contribution to k_{et} (i.e., a less negative value of $E - E^\circ$) at a given electrode potential (eq 3). The strong-field ammine ligands may also yield a larger intrinsic barrier for $Cr(NH_3)_5NCS^{2+/+}$ relative to $Cr(OH_2)_5NCS^{2+/+}$, thereby acting to further increase $(k_{et}^{OH_2}/k_{et}^{NH_3})_E$.

(28) Linck, R. G. *MTP Int. Rev. Sci.: Inorg. Chem., Ser. One* **1972**, *9*, 336–9.

(29) Christensen, R. J.; Espenson, J. H.; Butcher, A. B. *Inorg. Chem.* **1973**, *12*, 564.

However, it is anticipated that any interaction between the chromium center and the metal surface will be smaller in the Cr(II) successor state than in the Cr(III) precursor state, so that variations in K_p caused by alterations in the nonbridging ligands are anticipated to provide the predominant contribution to variations in $\Delta G_{et}°$. Inspection of the adsorption data in Table II reveals that the ratios $(K_p^{Ag}/K_p^{Hg})_E$ for complexes containing ammine and ethylenediamine nonbridging ligands are markedly (ca. 10- to 10^2-fold) smaller than those for aquo complexes having the same bridging ligand, although the values of K_p necessarily refer to potentials positive of the region where the kinetic data were gathered. In view of eq 4, given that $\alpha_{et} \approx 0.5$, the observed ca. 10- to 10^2-fold larger rate ratios $(k_{et}^{Ag}/k_{et}^{Hg})_E$ for the former reactants can therefore be accounted for at least in part by this "surface thermodynamic" contribution.

These differences in K_p at silver and mercury can be rationalized in terms of electronic interactions between the reactants and the metal surfaces. The perturbation upon the Cr(III) redox center induced by the silver electrode would be expected to be rather different from that brought about by the mercury surface, especially since at the electrode potential chosen for comparison (−600 mV) the former carriers a positive, and the latter a negative, excess electronic charge. (The pzc values at polycrystalline silver and mercury in 0.1 M $NaClO_4$ are −950[7] and −460 mV,[30] respectively.) The silver surface may significantly drain electron density from the nitrogen of the bridging thiocyanate, thereby weakening the $Cr(III)–NCS^-$ bond and yielding smaller values of K_p. Indeed, the values of K_p for $Cr(OH_2)_5NCS^{2+}$ and especially $Cr(NH_3)_5NCS^{2+}$ are markedly smaller than that for NCS^- at silver (Table II). This effect is also expected to diminish the intrinsic barrier ΔG_i^*, and hence increase k_{et}, since the $Cr(III)–NCS^-$ bond would then require less energy to be stretched. (Such bond stretching of a pair of trans ligands, presumably along the bridging axis, provides a major component of the intrinsic barrier for Cr(III) and Co(III) reductions.[28]) Another factor that may enhance the rate ratios $(k_{et}^{Ag}/k_{et}^{Hg})_E$ for the reduction of complexes containing ammine, ethylenediamine, or thiocyanate nonbridging ligands (Tables I and III) is the increase in ligand field stabilization energy that has been suggested to accompany the thiocyanate-bridged adsorption of Cr(III) and Co(III) at mercury electrodes.[19,31] Such an increase, attributed to greater chromium to ligand π bonding upon adsorption,[31] is in harmony with the larger values of K_p for $Cr(NH_3)_5NCS^{2+}$ compared to $Cr(OH_2)_5NCS^{2+}$ at mercury[19] (Table III); it would also yield larger intrinsic barriers ΔG_i^* and hence smaller values of k_{et} at mercury since the $Cr(III)–NCS^-$ bond would thereby be strengthened. This effect appears to be absent at silver electrodes, judging by the smaller values of K_p for $Cr(NH_3)_5NCS^{2+}$ than for $Cr(OH_2)_5NCS^{2+}$ (Table II).

Electron-Transfer Mediation by Bridging Ligands. Some of the data presented in Table I are also pertinent to the question addressed in the preceding article[2] regarding the manner and extent to which surface attachment of the reactant may alter the reorganization barrier to electron transfer. The reductions of $Cr(NH_3)_5Cl^{2+}$ and $Cr(NH_3)_5NCS^{2+}$ are of particular interest in this regard since the rates of their outer-sphere reduction at mercury are approximately known.[18,32] These rate data can be combined with estimates of K_p for the outer-sphere precursor states obtained from a suitable statistical model[2,3,33] to yield values of k_{et}^{est} for the outer-sphere reduction of $Cr(NH_3)_5Cl^{2+}$ and $Cr(NH_3)_5NCS^{2+}$ at mercury at −600 mV of ca. 10 and 2 s^{-1}, respectively.[33] The corresponding values of k_{et}^{est} for the inner-sphere pathways at mercury are similar (ca. 10 and 0.5 s^{-1}, respectively; Table I). Although the corresponding value of k_{et}^{est} for inner-sphere reduction of $Cr(NH_3)_5Cl^{2+}$ at silver (~100 s^{-1}; Table I) is markedly larger than both these corresponding values at mercury, this enhanced chloride-bridged reactivity at silver is not significantly greater than the corresponding enhancement in k_{et}^{est} seen for $Cr(NH_3)_5NCS^{2+}$. In other words, the relative values of k_{et}^{est} for $Cr(NH_3)_5Cl^{2+}$ and $Cr(NH_3)_5NCS^{2+}$ reduction are not greatly different at silver and mercury surfaces (Table I). This result contrasts that found for pentaamminecobalt(III) reduction at platinum and gold surfaces, where chloride was found to be a much more effective bridging ligand than thiocyanate in this regard.[2] The lack of additional catalyses seen for chloride-bridged reactions at silver may be associated with the relatively ionic character of the halide–silver bonding.[7]

Conclusions

The foregoing provides a demonstration of the differing influences that metal surfaces can exert on the energetics of ligand-bridged electrode reactions, arising from alterations in the energetics of the elementary electron-transfer step as well as in the stabilities of the precursor intermediates. For the most part, electrochemical kineticists have focused attention on the latter component so that the former contribution has usually been neglected. Similarly to the homogeneous intramolecular reactions involving binuclear metal complexes that have been extensively studied recently,[35] electrochemical systems involving surface-attached reactants clearly provide an important class of reactions with which to examine the energetics of the elementary electron-transfer step. Indeed, the latter systems have an important advantage in that the adsorbed reactant can be formed in a potential region where it is thermodynamically stable and, subsequently, be made suitably reactive by means of rapid alterations in the electrode potential. Another article expands the scope of the present electrochemical measurements to encompass heterogeneous electron mediation via extended organic bridges.[36]

Acknowledgment. Several items of electronic equipment were expertly designed and constructed by Marty Rabb. This work is supported by the Air Force Office of Scientific Research and the Office of Naval Research.

Registry No. $Cr(NH_3)_5NCS^{2+}$, 16884-60-9; $Cr(OH_2)_5NCS^{2+}$, 22258-89-5; $Cr(NH_3)_5N_3^{2+}$, 22317-10-8; $Cr(OH_2)_5N_3^{2+}$, 18517-09-4; $Cr(NH_3)_5Cl^{2+}$, 14482-76-9; $Cr(OH_2)_5Cl^{2+}$, 14404-08-1; $Cr(NH_3)_5Br^{2+}$, 22289-65-2; $Cr(OH_2)_5Br^{2+}$, 26025-60-5; *cis*-$Cr(OH_2)_4(NCS)_2^+$, 44965-83-5; *fac*-$Cr(OH_2)_3(NCS)_3$, 53539-42-7; $Cr(NCS)_6^{3-}$, 15276-09-2; *cis*-$Cr(en)_2(NCS)_2^+$, 25125-61-5; *cis*-$Co(en)_2(NCS)_2^+$, 21169-85-7; $NaClO_4$, 7601-89-0; Na_2SO_4, 7757-82-6; KF, 7789-23-3; NaF, 7681-49-4; Ag, 7440-22-4; Hg, 7439-97-6; NCS^-, 302-04-5; N_3^-, 14343-69-2.

---

(30) Parsons, R.; Payne, R. *Z. Phys. Chem.* (*Wiesbaden*) **1975**, *98*, 9.

(31) Baraclay, D. J.; Passeron, E.; Anson, F. C. *Inorg. Chem.* **1970**, *9*, 1024.

(32) Although $Cr(NH_3)_5NCS^{2+}$ reduction follows an inner-sphere pathway at mercury,[11] the kinetics of the corresponding outer-sphere pathway can be estimated approximately from the observed outer-sphere reduction rates of $Cr(NH_3)_5N_3^{2+}$.[18]

(33) From the "encounter preequilibrium" model for outer-sphere electron transfer, $k_{et}^{est} = k^{os}_{cor}/\delta r$, where k^{os}_{cor} is the work-corrected electrochemical rate constant (cm s^{-1}) for the outer-sphere pathway and δr is the effective reaction zone thickness at the electrode surface.[3] For Cr(III) ammine reductions at mercury, δr ~5 Å.[34] Inserting this along with experimental values of k^{os}_{cor}[11,18] into the above equation yields values of k_{et}^{est} at −600 mV of ca. 10 and 2 s^{-1} for $Cr(NH_3)_5Cl^{2+}$ and $Cr(NH_3)_5NCS^{2+}$, respectively.

(34) Hupp, J. T.; Weaver, M. J. *J. Phys. Chem.*, in press.

(35) For example, see: Haim, A. *Prog. Inorg. Chem.* **1983**, *30*, 273.

(36) Li, T. T-T.; Liu, H. Y.; Weaver, M. J. *J. Am. Chem. Soc.* **1984**, *106*, 1233.